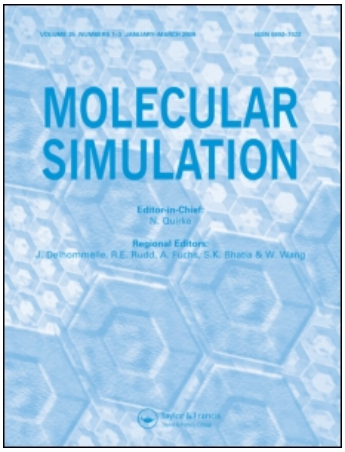

Molecular Simulation
Publication details, including instructions for authors and subscription information:
http://www.informaworld.com/smpp/title~content=t713644482

Molecular modeling study of sulfonated SIBS triblock copolymers

Jan Andzelm[ab]; James Sloan[b]; Eugene Napadensky[b]; Steven Mcknight[b]; David Rigby[c]
[a] Dynamics Science Inc., Aberdeen, MD, USA [b] Weapons and Materials Research Directorate, US Army Research Laboratory, Aberdeen Proving Ground, Aberdeen, MD, USA [c] Accelrys, Inc, San Diego, CA, USA

To cite this Article Andzelm, Jan , Sloan, James , Napadensky, Eugene , Mcknight, Steven and Rigby, David(2006) 'Molecular modeling study of sulfonated SIBS triblock copolymers', Molecular Simulation, 32: 2, 163 — 172
To link to this Article: DOI: 10.1080/08927020600728613
URL: http://dx.doi.org/10.1080/08927020600728613

Molecular Simulation, Vol. 32, No. 2, 15 February 2006, 163–172

Taylor & Francis
Taylor & Francis Group

Molecular modeling study of sulfonated SIBS triblock copolymers

JAN ANDZELM†‡*, JAMES SLOAN‡, EUGENE NAPADENSKY‡, STEVEN MCKNIGHT‡ and DAVID RIGBY¶

†Dynamics Science Inc., Aberdeen, MD, 21001, USA
‡Weapons and Materials Research Directorate, US Army Research Laboratory, Aberdeen Proving Ground, Aberdeen, MD, 21005-5069, USA
¶Accelrys, Inc, 10188 Telesis Ct., San Diego, CA, 92121, USA

(Received January 2006; in final form March 2006)

An important class of thermoplastic elastomers involves polystyrene and polyisobutylene blocks (SIBS). Sulfonated SIBS Triblock Copolymers (S-SIBS) are of particular interest because of potential applications for fuel cell and textile applications, where breathable, protective clothing is required. We have used multiscale modeling to gain an understanding of the static and dynamic properties of these polymer systems at detailed atomistic levels. Quantum chemistry tools were used to elucidate the bonding of water molecules and sulfonate groups. In addition, molecular dynamics was applied to calculate the polymer density at various levels of sulfonation. The structures of polymer with hydronium ions and also water were studied and the mechanism of water self-diffusion was proposed. It was found that with increase of water content the hydronium ions move further away from sulfonate groups. The self-diffusion coefficients of water were found to reproduce well experimental trends. Two different distributions of sulfonate groups were studied: one blocky and another perfectly dispersed. In the case of the blocky architecture, the water clusters are connected at a lower sulfonation level, leading to increased water diffusion coefficients as compared to the dispersed architecture.

Keywords: Multiscale modeling; Block copolymers; SIBS; Diffusion

1. Introduction

Microphase separated polymers exhibit unique properties useful in diverse types of applications. This is because the distinct phases may be optimized for different properties such as mechanical or permeative behavior resulting in a superior multifunctional material. We are particularly interested in multifunctional materials that can be applied to textiles as protective and breathable barriers. These materials would have two phases, one elastomeric phase that is impermeable but lightweight and flexible while the other ionic phase would have high water permeability. The ionic phase would form interconnected domains through the polymer and exhibit high selectivity defined as the ratio of permeability of water to that of organic solvent such as methanol or toxins.

One promising class of polymers is block copolymers, for example, polystyrene–polyisobutylene–polystyrene (SIBS) triblock copolymer [1,2]. The polyisobutylene component exhibits good barrier properties and also leads to low temperature flexibility of the material, while the polystyrene component allows for solvent permeability. Due to thermodynamic immiscibility of the two components spontaneous microphase separation occurs resulting in complicated morphologies, such as cylinders, lamellae or spheres [2,3], depending largely on the fraction of the polystyrene phase. The SIBS copolymer of interest in this work is comprised of approximately 30% polystyrene resulting in cylindrical (hexagonal) morphology. Upon sulfonation of the polystyrene repeat units, solvent permeability increases dramatically [4,5]. These phase segregated sulfonated polymers have hydrophilic domains containing the sulfonated groups, while the other phase is ion-deficient. At a particular sulfonation level, called the percolation threshold, the distinct hydrophilic domains become interconnected, thus allowing water and ions to pass through the polymer. In the case of SIBS it was found that the percolation threshold, characterized by a rapid increase in diffusion coefficients, is reached at about 20% of sulfonation [2,6]. In addition, increases in sulfonation level lead to increases in polymer density and particularly solubility [7].

These intriguing properties of sulfonated polymers are a function of their ordered ionic structures. Computational

*Corresponding author. Email: jandzelm@arl.army.mil

Molecular Simulation
ISSN 0892-7022 print/ISSN 1029-0435 online © 2006 Taylor & Francis
http://www.tandf.co.uk/journals
DOI: 10.1080/08927020600728613

studies to elucidate the relationship between polymer structure and transport properties of water have been performed mainly for an important fluoro-ionomer, Nafion [8–10]. These previous studies revealed that ions and water molecules are transported through the hydrophilic phase and that the structure of this phase directly impacts transport properties such as diffusion and conductivity. It was found that a polymer with short, polar side chains has higher water diffusivity than a longer-side-chain Nafion membrane [8]. The optimum distribution of the Nafion polar side chains was also determined using molecular dynamics simulations. Apparently, a higher water diffusion coefficient can be achieved by blocking together polar side chains [9]. The experimental and theoretical results on diffusion of water and hydronium ions in sulfonated membranes such as Nafion or polyether ketones (PEEK) was recently reviewed [11] and mechanism for water diffusion was proposed. With decreasing water content, the self-diffusion of water is retarded as a result of increasing confinement to narrow channels in polymer [11]. At higher water contents (i.e. >13 water molecules per sulfonic acid group in Nafion) water in the center of the channel exhibits bulk-like diffusion and permittivity [11,12] while close to the cavity surface water diffusion is significantly perturbed by the presence of the negatively charged sulfonic acid groups [13]. As long as the size of the channel does not fall below ~ 1 nm, the water at the center of the channels may still be bulklike [11,14]. A mechanism of water diffusion via hopping and vehicular motion was proposed in a polymer electrolyte study including poly(ethylene oxide) with sulfonic acid anion end groups [15].

The sulfonated block copolymers have been much less studied and we are not aware of computational studies done to elucidate effect of the polymer molecular structure on the transport properties. We have used a multiscale approach comprised of quantum, atomistic and mesoscale modeling [16]. The quantum chemistry modeling was used to deduce the atomistic model and to validate the force field describing atom-interactions, both necessary for the subsequent molecular dynamics simulations. The atomistic simulations allow us to explore basic relations between the molecular structure of SIBS and the mechanism of water self-diffusion. We determined the structure of copolymer with varying content of water and sulfonation levels focusing mostly on copolymers with a low sulfonation level, close to the percolation threshold. The morphology of SIBS and sulfonated SIBS polymer was studied using the mesoscale method and will be reported elsewhere [16].

2. Simulation details

2.1. Atomistic model

The system under consideration includes a sulfonated SIBS (S-SIBS) copolymer with water and counter ions such as hydronium or metal ions. In order to compare with experimental results we consider SIBS triblock copolymer as provided by Kuraray Co., Ltd., Tsukuba Research Laboratories with the reported properties; 30.84 wt% styrene, Mn 48,850 g/mol and specific gravity 0.95.

In this work, we have used an atomistic model including both polystyrene and polyisobutylene phases that is appropriate to study permeability at low sulfonation level and at the interface of two separated phases. In future work we will also consider another type of computational model that explicitly assumes a lamellar structure for S-SIBS copolymer which is more appropriate to study permeability at higher sulfonation level.

The general architectural pattern of our computational model is $R_nI_mR_n$, where R stands for a monomer (ring) of styrene and I is a monomer of isobutylene. Since the monomer weights are about 104 and 56 g/mol for styrene and isobutylene, respectively, one can calculate that the corresponding atomistic model should be approximately $R_{73}I_{602}R_{73}$. This estimation neglects the effect of polydispersity that is about 1.47. Use of a $R_{73}I_{602}R_{73}$ model would be computationally very expensive, therefore, for most of our calculations we adopted a smaller model $R_{14}I_{120}R_{14}$, that is approximately 1/5 of the size of a full model. Some tests with a larger model $R_{36}I_{300}R_{36}$ were also conducted and while some properties, notably polymer density, improved in comparison with experiment, we do not expect that use of such a large model would affect trends and general conclusions of this paper. We also assumed that the styrene block corresponds to atactic polystyrene with probability of chiral inversion set to 0.5.

Taking into account the experimental sulfonation procedure it can be expected that the sulfonated groups are attached in the *para* position of the styrene rings in the S-SIBS copolymer. Instead of modeling this random copolymer we have created two distinct models: (a) with evenly dispersed sulfonated groups, and (b) with blocked sulfonated groups. The real S-SIBS copolymer has a structure that is likely a superposition of our two models, although in the case of low sulfonation level, the dispersed architecture should be more preferred. In the case of the "blocky" architecture, we assumed the sulfonated blocks are localized at the end of a styrene block. Other distributions of sulfonated blocks will be studied in a forthcoming paper. Table 1 includes details of the content of our model as a function of sulfonation level used in an experimental study. Due to limited size of this model the sulfonation level only approximately matches experimental data; for example, to model system with experimentally determined 17% of sulfonation we use model marked as S-SIBS(17) that in fact includes close to 14% sulfonated groups. Larger models that match more precisely experimental data will be considered in a forthcoming paper.

The structures of a polymer specified in table 1 correspond to completely dehydrated polymer that is an idealized model of a real membrane. Since the annealing of a polymer membrane is done at 50°C [6,7], well below

Table 1. Architecture of S-SIBS(n) atomistic models for various sulfonation levels, *n*; I, R, S denote monomers of isobutylene, styrene and sulfonated styrene, respectively. Subscript numbers indicate number of monomers.

Model name	*Architecture*
SIBS(0)	$R_{14}I_{120}R_{14}$
Dispersed	
S-SIBS(17)	$S_1R_{12}S_1I_{120}S_1R_{12}S_1$
S-SIBS(22)	$S_1R_6S_1R_5S_1I_{120}S_1R_5S_1R_6S_1$
S-SIBS(29)	$S_1R_4S_1R_3S_1R_3S_1I_{120}S_1R_3S_1R_3S_1R_4S_1$
Blocky	
S-SIBS(17)	$S_2R_{12}I_{120}R_{12}S_2$
S-SIBS(22)	$S_3R_{11}I_{120}R_{11}S_3$
S-SIBS(29)	$S_4R_{10}I_{120}R_{10}S_4$

the water boiling point, it is very likely that there is water present even in so-called "dry" copolymer. The water content will be considered in the next section.

2.2. Interaction of water with sulfonated styrene

A realistic description of water in contact with sulfonated styrene in all S-SIBS model of membranes is of key importance to understand water permeability in those systems. We used the COMPASS force field [17] in molecular dynamics simulations of water diffusivity. This is an all-atom force field optimized to predict density and thermophysical properties for many common organic and inorganic molecules including polymers. The energy expression comprises many terms representing bonded interactions that were optimized using the *ab initio* (Hartree Fock) method. The non-bonded Coulombic interactions were found by considering electrostatic potentials from the *ab initio* calculations, whereas van-der Waals (vdW) forces was fitted to experimental data. Numerous applications of the COMPASS force field to polymers are reported in the literature [17,18]. However, COMPASS does not allow for bond breaking during molecular dynamics simulations and, therefore, we need to determine the bonding topology at the start of the simulations. Although the analysis of experimental vibrational spectra leaves some ambiguity as to the anionic or acidic form of the sulfonated group [7], it is reasonable to assume that at the temperatures S-SIBS polymer is cast, annealed and studied all the sulfonated groups are deprotonated.

We have studied the deprotonation reaction of sulfonic acid using small models of sulfonated polystyrene oligomer. We used the DMol density functional theory (DFT) [19] program at the PBE/DNP level that is known to provide accurate results of geometry and energetics for hydrogen-bonded systems [20]. Figure 1 shows geometry details of three water molecules bonded via hydrogen bonds to a sulfonated group in the *para* position of oligomer with 5 styrene rings (for clarity only one sulfonated group is shown). This water configuration spontaneously withdraws a proton from the sulfonated group forming a hydronium ion surrounded by two water

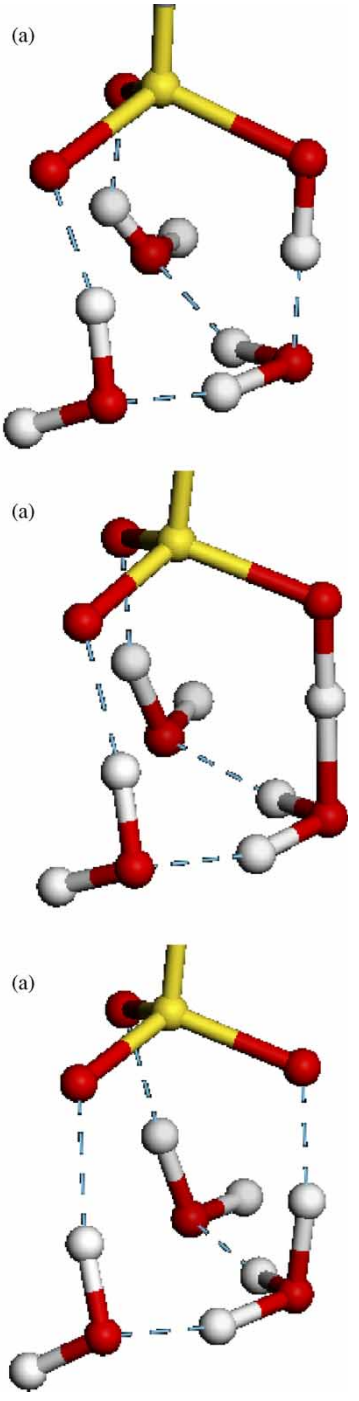

Figure 1. Snapshots from geometry optimization of a sulfonated group with neighboring three water molecules (a) start of optimization, (b) intermediate stage, (c) fully optimized structure as obtained by the DFT (PBE/DNP) method (details of molecular geometry can be sent upon request). In the online colour version the sulfur, oxygen and hydrogen atoms are marked with yellow, red and white, respectively.

molecules. Presence of only one or two water molecules is insufficient to deprotonate sulfonic acid—a similar conclusion already reported by considering deprotonation reaction in *p*-toluene sulfonic acid [21]. Increasing the number of waters molecules leads to moving the hydronium ion further from the sulfonated group. Based on this finding we selected a model for molecular dynamics calculations assuming the S-SIBS copolymer

with sulfonated groups in the anionic form is surrounded by water molecules and neutralized by hydronium ions. At least two water molecules have to be present per every sulfonate anion, even in the so-called dry form of S-SIBS copolymer. We performed calculations with 2, 6, *m* number of water molecules per sulfonate anion that correspond to dry, medium and fully saturated with water S-SIBS copolymer, respectively. To calculate the maximum number, *m*, of water molecules at full saturation we used the experimental solubility data [7] that provide the increase in the polymer mass upon hydration. Considering the polymer model as described in section 2.1 and molar mass of water of 18 g/mol, *m* is estimated to be: 12, 15 and 16 for sulfonation levels of 17, 22 and 29%, respectively. To identify calculated models we used a notation, such as, e.g. S-SIBS(17)-12 that shows a 17% sulfonation level with 12 water molecules per every sulfonate group, SO_3^-.

2.3. Details of atomistic simulations

Molecular dynamics simulations were performed using the Discover program from Materials Studio [22] with the COMPASS parameters [22,17]. To model the SO_3^- anion, we used "S4=" and "O" force field atom types for S and O atoms, respectively. The charge on the oxygen atoms was reassigned to -0.41 au in order to achieve a total charge of -1 au for the entire sulfonate group. The charge on oxygen atom of -0.41 au compares quite well with the atomic point charge of -0.44 au calculated from a fit to the electrostatic potential obtained from Dmol calculations [19] on a model structure presented in figure 1. The negative charge is balanced by the hydronium molecule and therefore, the total charge of the simulation cells is zero. The accuracy of this model was tested in calculations for S-SIBS oligomers with water and hydronium ion clusters. Structures were optimized using the DFT (PBE/DNP) approach and interaction energy was calculated using both DFT and the COMPASS force field. The average interaction energy (using six structures with up to five water molecules) was about 121 kcal/mol at the DFT level (calculated structures can be sent upon request). The COMPASS results are within 10% of the DFT results, which was considered satisfactory for the present purpose.

Initially, the bulk phases were constructed with the Amorphous Cell program of Materials Studio [22]. This program uses a Monte-Carlo technique to build an amorphous structure as a three-dimensional periodic cell. In order to avoid generation of high-energy configurations; the "lookahead" feature of the Amorphous Cell program was used with a value of 5. Every simulated system was optimized using five amorphous cell structures and the average values are reported. After each periodic cell was created, it was energy minimized followed by an extensive annealing procedure to equilibrate the system. The annealing procedure was found necessary to allow for proper distribution of water molecules in the unit cell. This procedure comprised of heating the system to 800 K for 50 ps followed by annealing in steps of 5 ps/50 K until room temperature of 298 K. The annealing procedure was repeated twice under NVT conditions (Andersen thermostat) [23]. Density determination using the NPT ensemble was carried out for at least 0.5 ns, until the density from the last 50 ps run was stable within 1%. For the NPT runs, the pressure was controlled using Berendsen's method [24] with pressure scaling constant set to 0.5 ps and system compressibility at 0.5 GPa. The equations of motion were integrated using the Verlet algorithm with a time step of 1 fs. During these simulations the cutoff for the non-bond interactions was taken as 9.5 Å with buffer width 0.5 Å. We have used the group-based non-bond summation method to improve the computation time. The appropriate number of hydronium ions precisely balanced the total, negative charge of such oligomer. The number of hydronium ions can be deduced from the table 1; for example, S-SIBS(17) oligomer has four sulfonated groups, S, hence 4 hydronium ions have to be used per every oligomer of this type. The number of water molecules used varied from two per SO_3^- group to model a dry polymer, to 12 for a fully solvated case (S-SIBS(17)-12).

3. Simulation results and discussion

3.1. Structure of sulfonated SIBS

It was experimentally observed that increasing the sulfonation level leads to a larger density of S-SIBS [4–7]. The calculated density for dry S-SIBS is presented in table 2 and it closely follows experimental results. Increasing the size of our model may improve agreement with experiment. In the case of SIBS copolymer, doubling the size of the model to $R_{36}I_{300}R_{36}$ led to increase in density from 0.926 to 0.935 g/cm^3 improving agreement with the experimental density of 0.95 g/cm^3.

However, increasing the number of oligomers in the unit cell had negligible impact on the calculated density. Calculated densities of isobutylene and polystyrene are 0.892 ± 0.003 and 1.033 ± 0.006 g/cm^3, respectively. This compares very well with experimental values [25,26] of 0.898 and 1.04–1.05 g/cm^3, respectively, indicating that interactions of methyl and also styrene groups are well described by the COMPASS force field. Thus the remaining error of about 2–3% could be attributed to the use of estimated force field parameters for the sulfonate group and its interaction with water, which were necessary since COMPASS does not currently have a full parameter set for this particular group.

Table 2. Density of a dry S-SIBS copolymer as a function of sulfonation level, (in g/cm^3).

Sulfonation level	*Simulations*	*Experiment [7]*
17	0.94 ± 0.01	0.97 ± 0.01
22	0.95 ± 0.02	0.99 ± 0.01
29	0.98 ± 0.02	1.03 ± 0.03

The results discussed in this section are representative of the dispersed architecture, which is most likely to dominate at low sulfonation levels. The blocky architecture density is within calculated errors close to simulated values from table 2.

A typical calculated structure is presented in figure 2 for S-SIBS(29) with 2, 5, 16 water molecules per sulfonated group. The structure (figure 2a) with two water molecules per SO_3^- group (plus hydronium ion) corresponds to dry S-SIBS. For clarity C and H atoms of isobutylene and polystyrene were removed. One can see that the water phase is segregated from the polymer. Water (and hydronium ions) linked with hydrogen bonds aggregate around sulfonated groups. In the case of low water content, water forms separated clusters connected with sulfonate groups through hydrogen bonds involving oxygen atoms of the SO_3^- group. Occasionally we can find a water molecule trapped within a polystyrene phase. At full solubility of 16 water molecules per each SO_3^- group, water forms continuous channels predominantly in two-dimensions, that may look like a lamellar structure. The alternative way of visualizing water channels is to calculate the surface accessible to solvent (SAS) assuming for water a radius of 1.4 Å. A continuous SAS indicates that a channel for transfer of water is open along the sulfonated groups. The SAS calculation was done by first removing water and hydronium from the structure. That creates a free volume of 1463 $Å^3$ using grid spacing of 0.4 Å. Next, a vdW surface was created assuming a probe radius of 1.0 Å and finally, a probe representing a solvent with radius of 1.4 Å was rolled over the externally accessible vdW surface to create a solvent accessible surface, SAS.

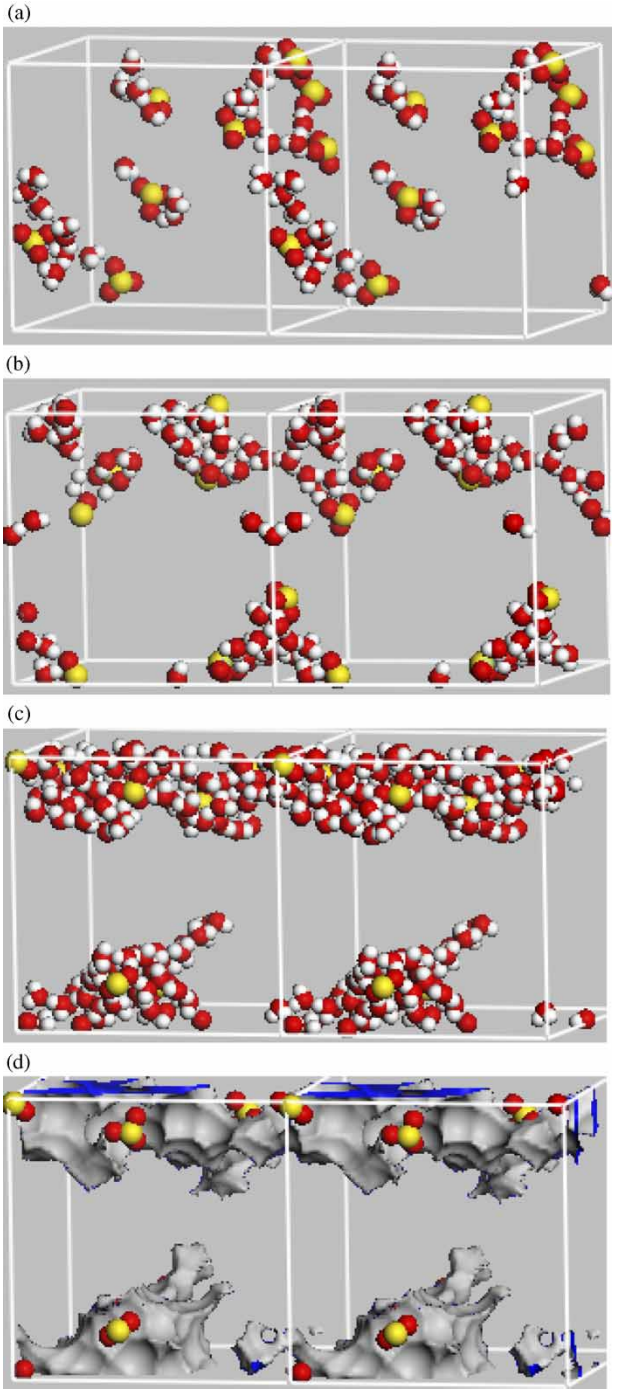

Figure 2. A snapshot from the MD simulations for model A, S-SIBS(29) with various content of water molecules per sulfonated group: (a) 2, (b) 5, and (c) 16. The sulfur, oxygen and hydrogen atoms are marked with yellow, red and white, respectively. The isobutylene and styrene fragments were removed for clarity. Figure (d) displays SAS with solvent probe radius of 1.4 Å.

We have calculated pair correlation functions to study structure with the thermal motion of atoms averaged from 1 ns of NVT simulations. An amorphous cell with density close to the average calculated value of density was used in these calculations. The pair correlation function, $g_{xy}(r)$ of two particles yields a probability of finding one particle, x from another one, y at a distance r apart relative to the probability of a random distribution of these particles. The $g_{xy}(r)$ was also integrated to provide the so-called coordination number, $n_{xy}(r)$ that indicates the number of particles y coordinated to the particle x within a radius r [9,15].

Figure 3 shows typical $g(r)$ graphs in the case of S-SIBS(29)-5 for the dispersed architecture. The distribution of water molecules is clearly correlated with sulfonated groups, represented here by a sulfur atom (figure 3a). We find one main coordination shell extending up to 4–4.5 Å. The position of water molecules with respect to the carbon atoms of a polymer is quite random. A more detailed examination of pair correlation functions involving carbon atoms from the styrene ring (figure 3b) reveals some degree of correlation particularly with the hydronium ions. This is likely due to the electrostatic interaction of quadrupole moments of the styrene ring with charged H_3O^+ ions residing in the neighborhood of sulfonated styrene rings. Both water and hydronium ions form hydrogen bonds with the oxygen atoms of each sulfonated group. On average hydrogen atoms from H_3O^+ are closer to oxygen at 1.55 Å while water forms hydrogen bonds at 1.65 Å.

The coordination numbers are presented as a function of distance between oxygen of the sulfonate group and hydrogen atoms of water (Os–Hw) and hydronium ion

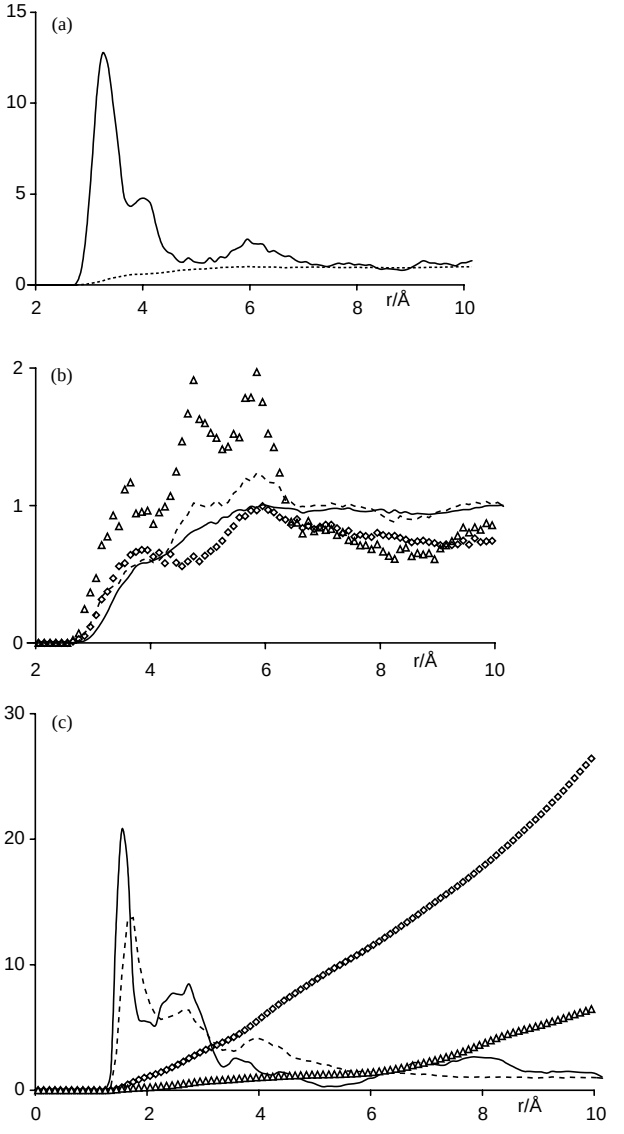

Figure 3. The pair correlation function of S-SIBS(29)-5, $g(r)$ between (a) the sulfur (—), carbon (- -) atom and the oxygen atom in water, (b) the carbon atom in styrene ring and oxygen atom in hydronium ion (△), water (◇); the carbon atom and oxygen atom in H_2O (—) and H_3O^+(- -) and (c) the oxygen atom of SO_3^- group and hydrogen atom in H_2O (—) and in H_3O^+(- -); the coordination numbers $n_{\text{water}}(r)$ (◇), $n_{\text{ion}}(r)$ (△).

(Os–Hi), respectively (figure 3c). Since there are five times as many H_2O molecules (40) as H_3O^+ ions (8) the $n(r)$ values for water are much larger. We find that about 35% of all water molecules and 43% of all hydronium ions are located within 10 Å from the oxygen of sulfonated group. The size of the unit cell is 26.75 Å in this case. The coordination number from the first coordination shell indicates the number of hydrogen atoms forming hydrogen bonds with the oxygen belonging to a SO_3^- group. In the case of the H_3O^+ ion the end of the first shell is clearly visible at 2.05 Å yielding a coordination number of $\sim$0.3. For the water molecules, the termination point for the first shell is more ambiguous and falls between 2.25 and 2.45 Å which leads to a coordination number of 1.6 ± 0.1. Clearly, there are more water molecules than H_3O^+ ions that can participate in hydrogen bonding with the SO_3^- group. According to our model which is based solely on distances, every oxygen atom can form multiple bonds with neighboring hydrogen atoms of water and hydronium ions.

Table 3. Coordination numbers as a function of sulfonation level (17, 22 and 29%) and water content[†]).

Sulfonation level, water content	*Os–Hw*	*Os–Hi*	*S–Ow*	*S–Oi*	*Oi–Ow*
17, 2	0.6	0.4	1.7	1.0	1.3
17, 5	1.2	0.3	3.4	0.8	2.5
17, 12	2.6	0.0	6.2	0.0	4.1
22, 2	0.6	0.3	1.6	1.2	1.6
22, 5	1.5	0.3	3.7	1.0	2.6
22, 15	2.6	0.1	7.2	0.3	3.9
29, 2	0.6	0.4	1.5	0.8	1.3
29, 5	1.6	0.3	3.4	0.6	2.3
29, 14	2.8	0.1	7.3	0.1	4.6

[†]Water content indicates the number of water molecules per sulfonate group. Results are given for the first coordination shell of the sulfonate group oxygen (Os) with hydrogen atoms of water (Hw), hydrogen of hydronium ion (Hi) and also oxygen atoms of ion (Oi) and water (Ow). Coordination numbers for S atom (S) were calculated with the coordination shell radius of 4.5 Å.

Table 3 summarizes the results of coordination numbers for three levels of sulfonation and solvation as calculated for the first coordination shell, typically terminated at a radius of 2.35 Å except in the case of sulfur–water (S–Ow) and sulfur–hydronium-ion (S–Oi) where the values of $n(r)$ are provided for a radius of 4.5 Å. This is the radius that typically ends the first coordination shell for the $g(r)$ of S–water. Using the same radius allows us to compare the distribution of water and ions at various levels of sulfonation and water content. Due to the ambiguity of selecting the termination radius in calculation of $n(r)$ values, the results reported in table 3 may differ by ± 0.1, nevertheless we expect the trends to be clearly indicated. Coordination numbers increase for both Os–Hw and S–Ow with the water content as expected. However unexpectedly, we also notice decreases in both the Os–Hi and S–Oi radial distribution. This indicates that additional water moves H_3O^+ ions away from sulfonated groups. The number of water molecules surrounding H_3O^+ ions increase significantly with the H_2O content according to the $n(r)$ Oi–Ow values in table 3. Hydronium ions, previously bonded to sulfonated groups are now bonded to water molecules via hydrogen bonds.

Figure 4 illustrates this phenomenon by comparing $g(r)$ and $n(r)$ values for the S-SIBS(29) case at two solvation levels with 2 and 16 water molecules/SO_3^- group, respectively. One can see that within the first coordination shell and up to 8 Å, there is a greater probability of finding hydronium ions close to the sulfonated group in the case of low water content. The second peak shown at about 9 Å could be interpreted as H_3O^+ hydronium ions associated with the next sulfonate group. The dominant intra molecular distance between sulfonate groups within the same polymer chain is about 9.5 Å. Thus the local environment of sulfonate groups as shown in table 3

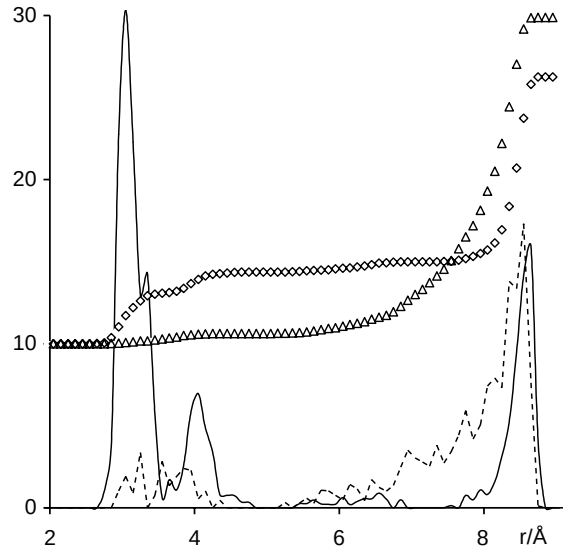

Figure 4. The pair correlation function, $g(r)$ of S-SIBS(29)-2 (—) and S-SIBS(29)-16 (- -) between S atom and oxygen atom of H_3O^+ ion. For clarity, the coordination numbers, n(r) for S-SIBS(29)-2 (◇) and S-SIBS(29)-16 (△) are multiplied by 5 and shifted upwards by 10.

seems to be largely unperturbed by the neighboring sulfonate groups which can explain relatively similar results for various sulfonation levels. In the case of higher sulfonation levels and blocky architecture, we should expect a larger impact from the neighboring sulfonate groups. An additional measure of the isolation of the sulfonate groups is the $g(r)$ value of Os–Os which clearly shows one peak at about 2.65 Å. This corresponds to the average distance between oxygen atoms of unperturbed SO_3^- group. The corresponding coordination number for Os–Os is calculated at 2.0 since every oxygen atom has only two neighbors in the SO_3^- group.

3.2. Diffusivity

To study the self-diffusion of water, diffusion coefficients D were calculated by fitting the Einstein equation to the long time (t) limit of the mean-squared displacement, $\langle r^2(t)\rangle$ (MSD) of water. This procedure is valid when the slope of log(MSD) vs. log(t) is close to 1. The MSD(t) curve consists of three regions: a short time ballistic part, with $\langle r^2(t)\rangle \sim t^2$, an anomalous region with $\langle r^2(t)\rangle \sim t^n$, $n < 1.0$ and the Fickian regime where $\langle r^2(t)\rangle \sim t$.

The Fickian regime corresponds to a random motion of water. Following recommendations in the literature [27, 28] we define the Fickian regime when the slope of the log(MSD) vs. log(t) curve is within 10% of 1.0. The MSD were calculated by analyzing a trajectory obtained from NVE molecular dynamics simulations of duration at least 4 ns. Nevertheless, we find it very difficult to satisfy this condition and successful runs require typically about 5 ns with the Fickian region appearing from 3.6 to 4.6 ns. In the case of low water content, no Fickian region was found even after 6 ns MD runs. Results reported in this paper correspond to full water saturation, which amounts to 15 water molecules per sulfonate group in the case of the 22% sulfonation level.

Table 4. Average, maximum and minimum displacement, distance traveled and absolute value of jump for water molecules in the S-SIBS(17)-12 and S-SIBS(22)-15 model (in Å)[†].

Water movement	*S-SIBS(17)-12*	*S-SIBS(22)-15*
Distance traveled (T)		
Average	214	244
Maximum	268	323
Minimum	86	122
Displacement (S)		
Average	9.9	11.4
Maximum	26.1	36.2
Minimum	0.9	0.8
Jump		
Average	2.1	2.4
Maximum	10.5	13.7

[†]Averaging was done using 48 and 90 water molecules for the S-SIBS(17)-12 and S-SIBS(22)-15 model, respectively.

The trajectories of individual water molecules were examined to characterize the diffusion mechanism. The Fickian regime from 3.6 to 4.6 ns was divided into 10 ps time blocks and positions of all waters were compared at the end of each block. This allows us to calculate the total distance water traveled and the displacement between its original and final position. The displacement within each time block is considered here as a jump movement.

Table 4 presents results for typical S-SIBS(17)-12 and S-SIBS(22)-15 diffusion calculations. One can see that water molecules travel a significant distance, on average about 240 Å; although within 1 ns the average total displacement is less than half of the size of the periodic amorphous cell. There are 61% water molecules that travel further than the average molecule and about 40% that finish at a separation larger than the average displacement. There are some molecules trapped in the polymer matrix and typically the one with the largest distance traveled also shows the largest displacement.

Figure 5 shows the history of jumps for a molecule with the largest jump from the S-SIBS(22)-15 model. This figure shows the absolute values of jumps; in fact water jumps back and forth between different voids and hence the total displacement is much smaller than the distance traveled. It is interesting to compare a distribution of jump lengths with water movement in pure water. A unit cell with 90 water molecules was optimized and statistics were gathered over a period of 500 ps in steps of 10 ps. The jump distances were collected and averaged over the number of time blocks and number of water molecules. A similar procedure was also applied in the case of the polymer studied here and compared with pure water in figure 6. In the case of pure water one can find a broad distribution of jump-length probability, while in bulk polymer the probability is sharply peaked. Clearly water movement in ionomer is hindered by confinement to narrow channels in polymer and also by strong interaction

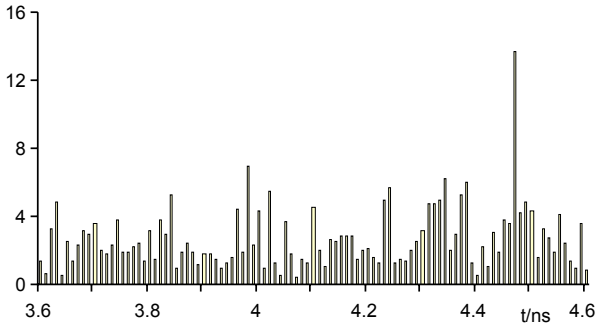

Figure 5. Histogram (—) of jump lengths (in Å) for a single water in S-SIBS(22)-15 of blocky architecture. The jump distance is calculated between successive positions of water measured at 10 ps intervals in the Fickian region. The average jump length is 2.4 Å.

with ionized sulfonic acid groups as will be discussed more in the next section.

3.3. Effect of polymer architecture on transport properties.

The self-diffusion coefficients (D) of water were calculated for both dispersed and blocky architecture of S-SIBS at 17 and 22% sulfonation levels. The model is defined in table 1 and the procedure for calculating the diffusion coefficient (D) was explained in section 3.2. In the case of S-SIBS(17)-12 model the values of D coefficients (in 10^{-6} cm^2/s units) are 1.2 ± 0.7 and 1.6 ± 0.6 for dispersed and blocky architecture, respectively, while in the case of S-SIBS(22)-15 model we obtained D equal to 1.7 ± 0.5 and 2.4 ± 0.6, respectively. These values are comparable to experimental measurement of about 0.5 and 1.0 for 17 and 22% sulfonation levels, respectively [6]. The overestimation in D values is likely due to several factors. First our model includes a water amount corresponding to the experimental solubility value, while experimental measurement of D is done at much smaller water content. The computational procedure used in this paper (force field, parameters of molecular dynamics simulations such as details of nonbond cutoff methods, etc.) introduces an error that is evident in calculation of D for pure water. For pure water, our simulations yield $D=3.6\times10^{-5}$ cm^2/s, while experimental values were reported at 2.3×10^{-5} cm^2/s [29]. Finally, in the case of S-SIBS(17) model, we were able to utilize only two or three cells (instead of 5), because the Fickian region was not achieved even after 7 ns of NVE simulations. Hence, the uncertainty of results is relatively large and the difference between the two architectures is not as meaningful as in the case of S-SIBS(22) where five cells were used.

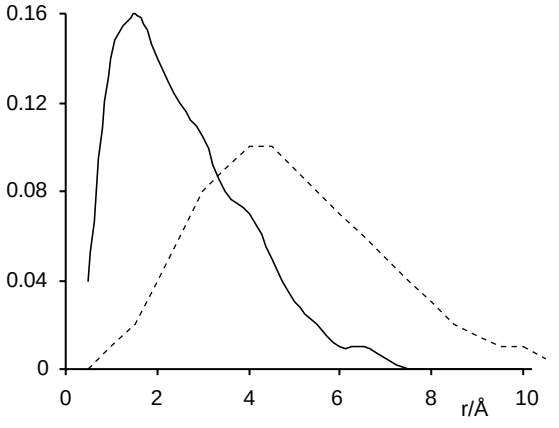

Figure 6. The distribution of jump lengths for a water in S-SIBS(22)-15 of blocky architecture (—) compared with that of pure water (- -).

Nevertheless, the present results indicate that the blocky architecture leads to higher diffusion coefficients as compared with the dispersed architecture. We can observe increases in averaged distance traveled, displacement and jump size for water in the blocky architecture of S-SIBS(22) as compared to the dispersed architecture. Apparently larger cavities with water can be formed for the blocky case allowing for less restricted water movement. The distribution of water molecules was quantified by plotting radial distribution functions and coordination numbers (figure 7) for both blocky and dispersed architecture of S-SIBS(22)-15. Within the first shell of each sulfur atom (to about 3 Å) both architectures show a similar water distribution. The water content is consistently larger at distances further from sulfur, and within a 12 Å radius there are approximately 55 and 43 molecules of water for the blocky and dispersed, architecture, respectively (this means there is about 30% more water molecules in the proximity of sulfur atoms). Figure 7b shows the sulfur–water distribution function, indicating that beginning from about 6 Å, the blocky architecture yields larger water clusters. The number of water neighbors within the shell from 6 to 12 Å is 40.1 and 31.5 for the blocky and dispersed architectures, respectively.

A plot of surface accessible to water (SAS) can serve as a qualitative visualization of water channels in the swollen polymer. For S-SIBS(17) SAS were calculated for blocky (figure 8a) and dispersed (figure 8b) architectures at various probe radii close to 1.4 Å, that is commonly used as a radii for a water molecule [30]. At a probe radius of 1.48 Å a clearly visible discontinuity of the SAS surface appears for the dispersed architecture. In the case of the blocky architecture, at the same radius of 1.48 Å, a continuous SAS exists indicating the opened channel for water diffusion. The difference in SAS pictures could be interpreted as indication of reaching a lower percolation threshold for the blocky architecture. The SAS plots could also be used to approximately measure the size of the channel at its most narrow point. Using a probe radii of 1.4 Å we estimate this critical diameter of a channel to be $\sim$3 and $\sim$1.5 Å for blocky and dispersed, architecture, respectively. The distribution of dielectric constant in channels less than 10 Å (1 nm) was found to be much smaller than for the bulk water [11–14] due to substantial interference of sulfonate ions. As channels found in this paper are much smaller than 1 nm, we conclude that water mobility is restricted by both narrow channels confinement and electrostatic interactions with sulfonate groups.

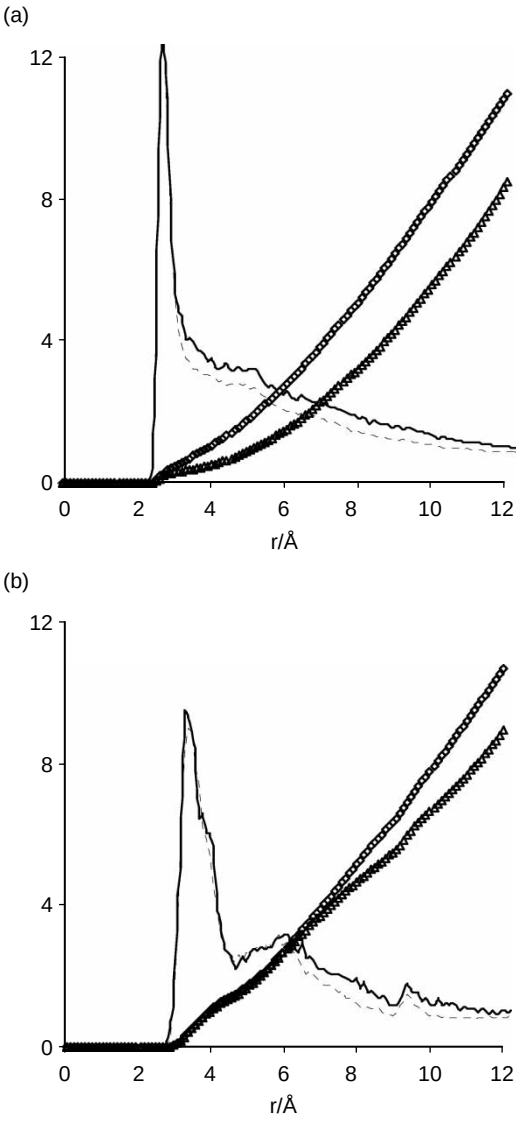

Figure 7. The pair correlation function, $g(r)$ of S-SIBS(22)-15 between (a) oxygen atoms of water, and (b) S atom and oxygen atom of water for the dispersed (- -) and blocky (—) architecture*). (* The g(r) is calculated by analysing data in the Fickian regime; from 3.6 ns to 4.6 ns is simulation time. For clarity, the coordination numbers, n(r) for the dispersed (△) and blocky (◇) architecture are divided by 5).

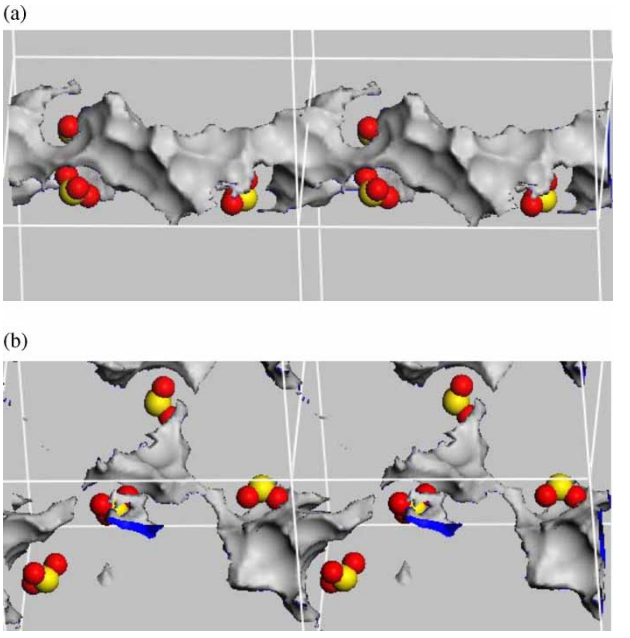

Figure 8. SAS with radius of 1.48 Å for S-SIBS(17)-12 model of (a) blocky, (b) dispersed SIBS at 17% of sulfonation.

4. Conclusions

In this work an atomistic model for sulfonated SIBS copolymer was proposed and verified in calculations at various levels of sulfonation and water content. We have found that three water molecules are necessary to withdraw a proton from sulfonic group. This allowed us to consider a model with SO_3^- groups in the *para* position of styrene neutralized with hydronium ions. Both water and hydronium ions are linked through hydrogen bonds and reside in the neighborhood of sulfonated groups. Simulations clearly result in a phase separation between ionic phase (SO_3^-, H_3O^+ and H_2O) and non-ionic region consisting of polyisobutylene and unsulfonated polystyrene groups. Dry S-SIBS may contain up to two water molecules/SO_3^- in clusters surrounding sulfonated groups, separated from each other by non-ionic phase. Increasing both the sulfonation and water content causes these clusters to grow and combine into channels allowing for water transport. The hydronium ions have a tendency to come closer to sulfonate groups and styrene rings at the low solvation level, while at higher water content they seem to move away from the sulfonate groups and reside surrounded by a pool of water. Both dispersed and blocky architecture show lamellar-type structure of water molecules linked to the sulfonate groups. This agrees with experimental results [2–7] and proves that our atomistic model of polymer is sufficiently large to describe that morphological feature of S-SIBS.

We have found that the calculated self-diffusion coefficients of water reproduce experimental trends, measured at 17 and 22% of sulfonation. It is challenging to reach a Fickian region for the systems studied here, leading to the necessity of using number of water molecules that correspond to a full solubility [7]. We found a well resolved jump distribution indicative of the hopping mechanism for self-diffusion with a jump-length distribution quite different from that of pure water. This is more typical of a solid-type hopping behavior than the diffusive movement in a liquid.

We have studied two different types of sulfonated group distributions: blocky and dispersed architecture. Although the experimental conditions lead to a random distribution of SO_3^- groups, we expect our dispersed architecture may be a better approximation of the real polymer. We found the self-diffusion coefficients to be consistently larger for the blocky architecture, particularly in the case of 22% sulfonation. We can construct a "surface accessible to water" by choosing the appropriate water-radius parameter that yields a continuous SAS display for the blocky case, while the SAS surface is broken for the dispersed

architecture. This could be interpreted as a capability of the blocky architecture to open channels for water diffusion. Comparison of the pair correlation functions for both architectures reveals formation of larger water clusters localized further from the sulfonate groups (at 6 Å, see figure 7). The diffusion of water molecules is not localized exclusively within these water cavities since water molecules can transfer from one cluster to another as indicated by an average displacement distance ($\sim$10 Å, see table 4) that is larger than the distance between clusters. The average displacement distance of water molecules is about 30% larger for the blocky architecture and that coincides with higher self-diffusion coefficient and further supports our conclusion about improved water transport in blocky polymer. We found that the blocky architecture at 17% sulfonation leads to diffusion coefficients comparable to those at 22% sulfonation for the dispersed architecture. We conclude that the blocky architecture achieves a percolation threshold at lower sulfonation level than one necessary for a dispersed architecture. Therefore, it might be beneficial to synthesize polymer with sulfonated groups precisely blocked within the polystyrene phase.

References

[1] R.F. Storey, B.J. Chisholm, Y. Lee. Synthesis and mechanical properties of poly(styrene-*b*-isobutylene-*b*-styrene) block copolymer ionomers. *Polym. Eng. Sci.*, **37**, 73 (1997).

[2] D.M. Crawford, E. Napadensky, N.C.B. Tan, D.A. Reuschle, D.A. Mountz, K.A. Mauritz, K.S. Laverdure, S.P. Gido, W. Liu, B. Hsiao. Structure/property relationships in polystyrene–polyiosbutylene–polystyrene block copolymers. *Thermochim. Acta*, **367**, 125 (2001).

[3] X. Lu, W.P. Steckle, R.A. Weiss. Ionic aggregation in a block copolymer ionomer. *Macromolecules*, **26**, 5876 (1993).

[4] Y.A. Elabd, E. Napadensky, J.M. Sloan, D.M. Crawford, C.W. Walker. Triblock copolymer ionomer membranes Part I. Methanol and proton transport. *J. Membr. Sci.*, **217**, 227 (2003).

[5] Y.A. Elabd, C.W. Walker, F.L. Beyer. Triblock copolymer ionomer membranes Part II. Structure characterization and its effects on transport properties and direct methanol fuel cell performance. *J. Membr. Sci.*, **231**, 181 (2004).

[6] E. Napadensky D. Crawford J. Sloan N.C.B. Tan Viscoelastic and transport properties of sulfonated PS–PIB–PS block copolymers ARL-TR-2482 Army Research Laboratory Proceedings (2001).

[7] Y.A. Elabd, E. Napadensky. Sulfonation and characterization of poly(styrene–isobutylene–styrene) triblock copolymers at high ion-exchange capacities. *Polymer*, **45**, 3037 (2004).

[8] R. Jimmouchi, K.J. Okazaki. Molecular dynamics study of transport phenomena in perfluorosulfonate ionomer membranes for polymer electrolyte fuel cells. *Electrochem. Soc.*, **150**, E66 (2003).

[9] S.S. Jang, V. Molinero, T. Cagin, W.A. Goddard. Nanophase-segregation and transport in nafion 117 from molecular dynamics simulations: effect of monomeric sequence. *J. Phys. Chem B*, **108**, 3149 (2004).

[10] D. Rivin, G. Meermeier, N.S. Schneider, A. Vishnyakov, A.V. Neimark. Simultaneous transport of water and organic molecules through polyelectrolyte membranes. *J. Phys. Chem. B*, **108**, 8900 (2004).

[11] K.D. Kreuer, S.J. Paddison, E. Spohr, M. Schuster. Transport in proton conductors for fuel-cell applications: simulations, elementary reactions and phenomenology. *Chem. Rev.*, **104**, 4637 (2004).

[12] R. Paul, S.J. Paddison. A statistical mechanical model for the calculation of the permittivity of water in hydrated polymer electrolyte membrane pores. *J. Chem. Phys.*, **115**, 7762 (2001).

[13] S.J. Paddison, R. Paul, K.D. Kreuer. *Phys. Chem. Chem. Phys.*, **4**, 1151 (2002).

[14] M. Ise. Thesis, University of Stuttgart, Stuttgart (2000).

[15] J. Ennari, I. Neelov, F. Sundholm. Estimation of the ion conductivity of a PEO-based polyelectrolyte system by molecular modeling. *Polymer*, **42**, 8043 (2001).

[16] J. Andzelm J. Sloan E. Napadensky S. McKnight D. Rigby Multiscale modeling of SIBS and sulfonated SIBS copolymers Proceedings AIChe Annual meeting (2005).

[17] D. Rigby, H. Sun, B.E. Eichinger. Computer simulations of poly(ethylene oxide): force field, PVT diagram and cyclization behavior. *Polym. Int.*, **44**, 311 (1997).

[18] T. Spyriouni, C. Vergelati. A molecular modeling study of binary blend compatibility of polyamide 6 and poly(vinyl acetate) with different degrees of hydrolysis: an atomistic and mesoscopic apporach. *Macromolecules*, **34**, 5306 (2001).

[19] B. Delley. From molecules to solids with DMol3 approach. *J. Chem. Phys.*, **113**, 7756 (2000).

[20] J. Andzelm, N. Govind, G. Fitzgerald, A. Maiti. DFT study of methanol conversion of hydrocarbons in a zeolite catalyst. *Int. J. Quantum Chem.*, **91**, 467 (2003).

[21] S.J. Paddison. The modeling of molecular structure and ion transport in sulfonic acid based ionomer membranes. *J. New Mater. Electrochem. Syst.*, **4**, 197 (2001).

[22] Materials Studio 3.2 (Discover, Amorphous Cell, COMPASS), Accelrys Inc, San Diego, CA, USA (Materials Studio 3.2).

[23] H.C. Andersen. Molecular dynamics simulations at constant pressure and/or temperature. *J. Chem. Phys.*, **72**, 2384 (1980).

[24] H.J.C. Berendsen, J.P.M. Postma, W.F. van Gunsteren, A. DiNola, J.R. Haak. Molecular dynamics with coupling to an external bath. *J. Chem. Phys.*, **81**, 3684 (1984).

[25] J. Brandrup, E.H. Immergut (Eds.), *Polymer Handbook*, John Wiley & Sons, New York (1975).

[26] C.R. Schultheisz, S.D. Leigh. NIST Special publication 260-143, Gaithersburg (2002).

[27] J.H.D. Boshoff, R.F. Lobo, N.J. Wagner. Influence of polymer motion topology and simulation size on penetrant diffusion in amorphous, glassy polymers: diffusion of helium in polypropylene. *Macromolecules*, **34**, 6107 (2001).

[28] S. Neyertz, D. Brown. Influence of system size in molecular dynamics simulations of gas permeation in glassy polymers. *Macromolecules*, **37**, 10109 (2004).

[29] R. Mills. Self-diffusion in normal and heavy water in the range 1–45 deg. *J. Phys. Chem.*, **77**, 685 (1973).

[30] M.L. Connolly. *Science,* 221 (1983).